

Sensor and Simulation Notes

Note 379

May 1995

**Impulse Radiating Antennas With Two  
Refracting or Reflecting Surfaces**

Everett G. Farr  
Farr Research

Carl E. Baum  
Phillips Laboratory

**Abstract**

We consider here a class of Impulse Radiating Antenna that uses two surfaces to direct the aperture field rays into a plane wave. Such designs can have a number of advantages over classical reflector or lens IRAs which use only a single surface. These new designs can reduce the total volume of an antenna, for a given level of high-frequency performance. These designs can also be used to achieve better and/or more flexible impedance matching to a source.

The designs discussed here include the Reflector Lens IRA (ReLIRA), the Split IRA (SPIRA) and the Cassegrain IRA (CasIRA). The ReLIRA is discussed for reflectors of planar, paraboloidal and hyperboloidal shapes, and for lenses of planar and prolate spheroidal shapes. The SPIRA is a technique for combining two half IRAs (HIRAs) into a transmit/receive pair. The CasIRA is a technique for combining a hyperboloidal subreflector with a large paraboloidal main reflector.

## I. Introduction

Impulse Radiating Antennas have by now become familiar in the art of radiating short impulses. First proposed in [1], their characteristics have been summarized in two summary papers [2-3], and numerous detailed papers [4-15]. Sketches of the two most commonly used IRAs, the reflector IRA and the lens IRA are shown in Figure 1.1. Recently, some new configurations have been suggested in [16]. In this note we propose a number of additional IRA configurations that use two reflecting or refracting surfaces.

To develop new IRA designs, we combine various well-established techniques for converting spherical waves to plane waves. This can be accomplished either with lenses [17-22] or reflectors [23-25]. The Reflector Lens IRA (ReLIRA) uses a single reflector and a single lens to convert a spherical wave to a plane wave. The Split IRA (SPIRA) uses two half IRAs to provide separate transmit and receive channels for a radar. Finally, the Cassegrain IRA (CasIRA) uses two reflectors to achieve a spherical wave.

By implementing these new techniques, one can build antennas that use less total volume than would otherwise be necessary. One can also achieve certain interesting input impedances, in one case with a SPIRA, exactly matching to a standard  $50 \Omega$  line. We begin now with the ReLIRA.

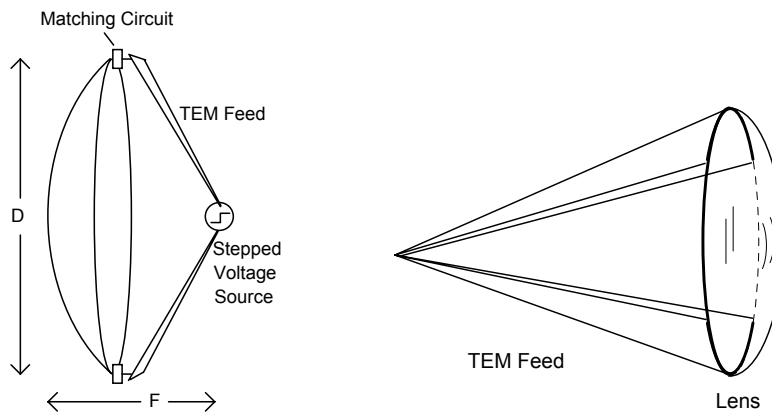


Figure 1.1. A reflector IRA (left) and a lens IRA (right).

## II. ReLIRA #1: Plane Reflector with Prolate Spheroidal Lens

The simplest version of the ReLIRA is sketched in Figure 2.1. Instead of using a paraboloidal reflector, one uses a planar reflector, which is fed by a conical pair of feed arms. The entire structure is embedded in a dielectric medium, and there is a prolate spheroidal lens [20, Section 3] to focus the rays for radiation into free space. Note that a prolate spheroid is just an ellipse that has been rotated around its major axis. The dielectric material might be a liquid, such as oil, or it might be a solid that has hardened from a liquid form.

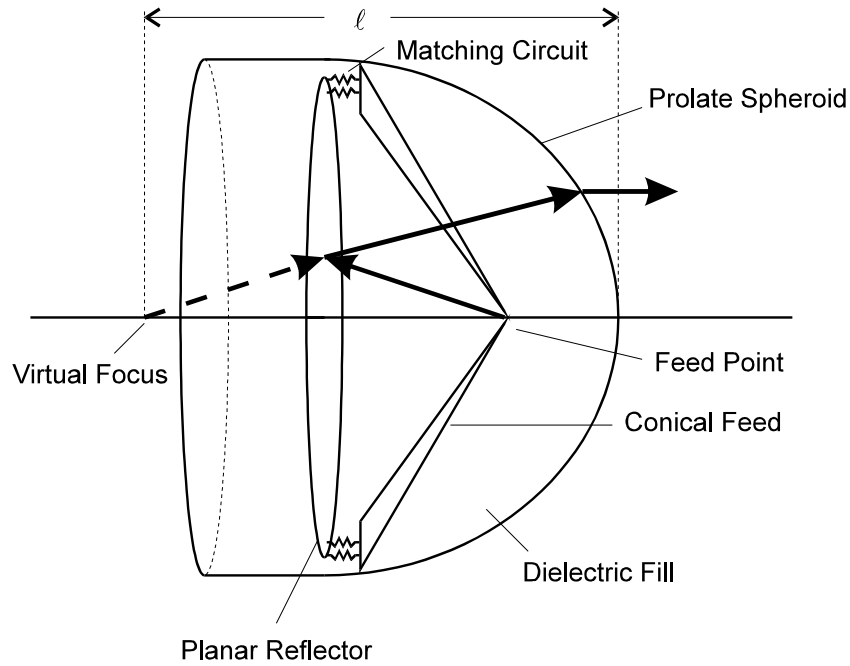


Figure 2.1. ReLIRA with Planar Reflector and Prolate Spheroidal Lens, two-arm version.

A sketch of a radial slice through the lens is shown in Figure 2.2. Note that we denote the radial cylindrical coordinate as  $\Psi$ , where many other authors use  $\rho$ . We do so in order to avoid a possible conflict in meaning of  $\rho$  to indicate charge density.

Let us now derive the equations describing the surface. In the  $\Psi$ - $z$  plane the equation of the surface is derived by comparing the electric lengths of the two ray paths shown in Figure 2.2. Thus, from transit-time considerations we have [20]

$$\sqrt{\varepsilon_1} \ell = \sqrt{\varepsilon_1} r + \sqrt{\varepsilon_2} (-z) \quad (2.1)$$

Let us now make the substitution

$$q = \sqrt{\varepsilon_2 / \varepsilon_1} \quad (2.2)$$

Typically, the value of  $q$  is between zero and one, however this is not a strict requirement. If  $q$  is greater than one, the surface that is generated is not a prolate spheroid, but a hyperboloid. Next, we expand  $r$  in its  $z$  and  $\Psi$  components as

$$r^2 = (\ell + z)^2 + \Psi^2 \quad (2.3)$$

Combining the above three equations we have

$$(\ell + z)^2 + \Psi^2 = (\ell + qz)^2 \quad (2.4)$$

This is the equation to be solved to determine the location of the ellipse in the  $\Psi$ - $z$  plane.

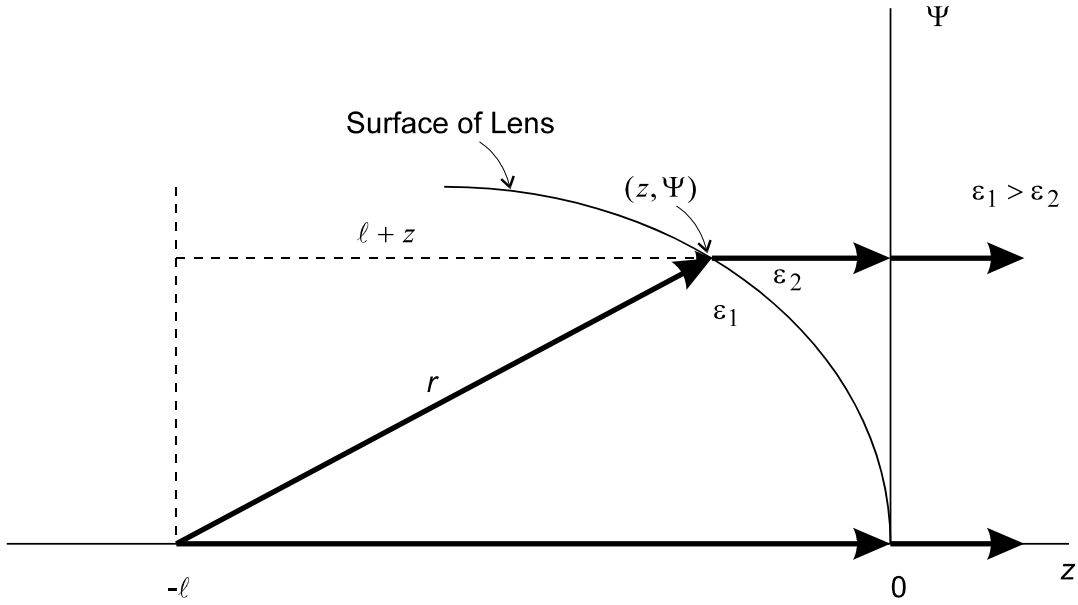


Figure 2.2. Geometry of the prolate spheroid dielectric interface (an ellipse when projected into the  $\Psi$ - $z$  plane).

Continuing from the above equations, we can simplify the description of the surface still further. With some rearrangement, including completing the square, we find

$$z^2 + \frac{2\ell}{1+q}z + \frac{\Psi^2}{1-q^2} = 0 \quad (2.5)$$

$$\left(z + \frac{\ell}{1+q}\right)^2 + \frac{\Psi^2}{1-q^2} = \frac{\ell^2}{(1+q)^2}$$

If we now make the substitutions

$$a = \frac{\ell}{1+q}, \quad b = \ell \sqrt{\frac{1-q}{1+q}} \quad (2.6)$$

we arrive at the final equation

$$\frac{(z+a)^2}{a^2} + \frac{\Psi^2}{b^2} = 1 \quad (2.7)$$

This equation is immediately recognizable as a simple ellipse with major axes of  $a$  and  $b$ , and offset in the  $z$  direction by  $-a$ .

At this point, it is helpful to plot the ellipse in more detail, as is shown in Figure 2.3. If one plots  $\Psi$  versus  $z+a$ , the ellipse is centered at the planar reflector, where  $z+a=0$ . The foci are located at  $z+a = \pm c$ ,  $\Psi=0$ . The focal distance  $c$  is determined by the usual formula for an ellipse [26],

$$c = \sqrt{a^2 - b^2} = \frac{\ell q}{1+q} \quad (2.8)$$

$$\ell = a + c \quad (2.9)$$

Note that the shape of the ellipse is determined once the two dielectric constants are chosen. This is made clear when the parameters are expressed more simply as

$$\frac{b}{a} = \sqrt{1-q^2}, \quad \frac{c}{a} = q \quad (2.10)$$

For typical values of  $\epsilon_1 = 2.25 \epsilon_0$  (oil or polyethylene) and  $\epsilon_2 = \epsilon_0$  (air), we have  $b/a = 0.745$  and  $c/a = 0.667$ .

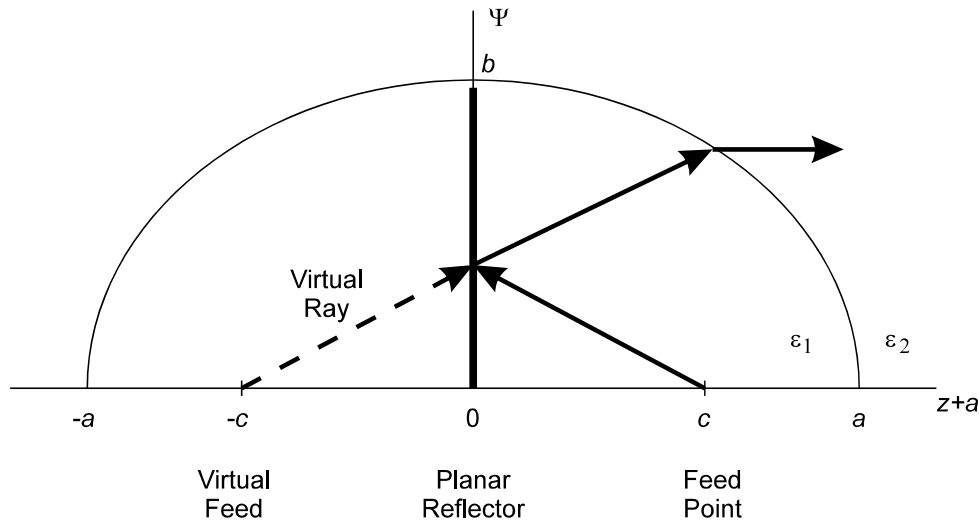


Figure 2.3. The ellipse used to generate the prolate spheroid for the lens surface.

Let us consider now the field radiated from such a device. If the device were not filled with dielectric, the far portion of the radiated field would be expressed as [1, 2-3, 5]

$$E_{rad}(r,t) = \frac{D}{4\pi r c f_g} \frac{dV(t)}{dt} \quad (2.11)$$

where  $D$  is the diameter of the reflector,  $r$  is the distance out to the observation point on the boresight axis,  $c$  is speed of light in free space, and  $V(t)$  is the driving voltage. Furthermore,  $f_g$  is the normalized feed impedance in the dielectric medium where  $f_g = Z_c/Z_o$ ,  $Z_c$  is the feed impedance, and  $Z_o$  is the impedance of free space. Since the antenna is embedded in a dielectric, we have to adjust this by a transmission coefficient

$$\tau = \frac{2Z_2}{Z_1 + Z_2} = \frac{2\sqrt{\epsilon_1}}{\sqrt{\epsilon_2} + \sqrt{\epsilon_1}} = \frac{2}{q+1} \quad (2.12)$$

Therefore the radiated field becomes

$$E_{rad}(r,t) = \frac{\tau D}{4\pi r c f_g} \frac{dV(t)}{dt} \quad (2.13)$$

Note that this adjustment for a transmission coefficient can only be considered approximate, since our expression for the transmission coefficient assumes normal incidence everywhere. In fact, the actual transmission coefficient varies locally with the angle of incidence. It may be of use in later work to calculate the radiated field more accurately by taking this into account.

Finally, we note a perturbation on this theme is the so-called Solid Dielectric Lens IRA. This combines a TEM horn embedded in a dielectric, with a prolate spheroidal lens interface. A sketch of this configuration is shown in Figure 2.4. Note that the feed point of the TEM horn is located at a focus of the prolate spheroid.

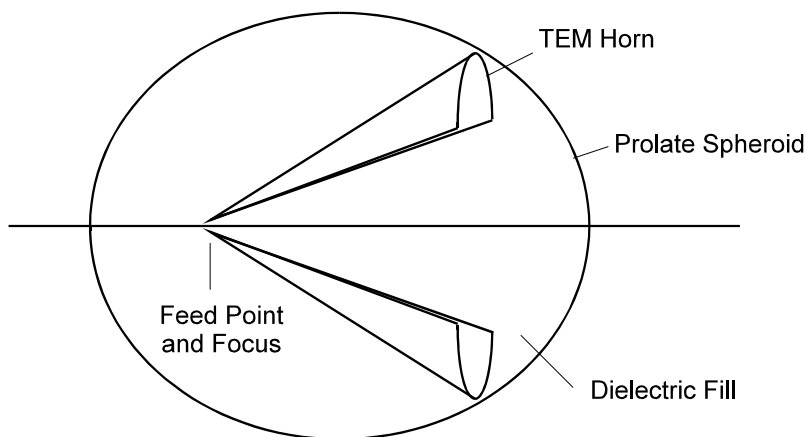


Figure 2.4. A solid dielectric lens IRA.

### III. ReLIRA #2: Hyperboloidal Reflector with Prolate Spheroidal Lens

Instead of using a flat plate as a reflector, one could also use one sheet of a hyperboloid of two sheets. In doing so, one converts the incident spherical wave into another spherical wave whose center is a different distance from the reflector. A diagram of such a configuration is shown in Figure 3.1. As before, the entire antenna would be encased in dielectric, with a prolate spheroidal lens at the output.

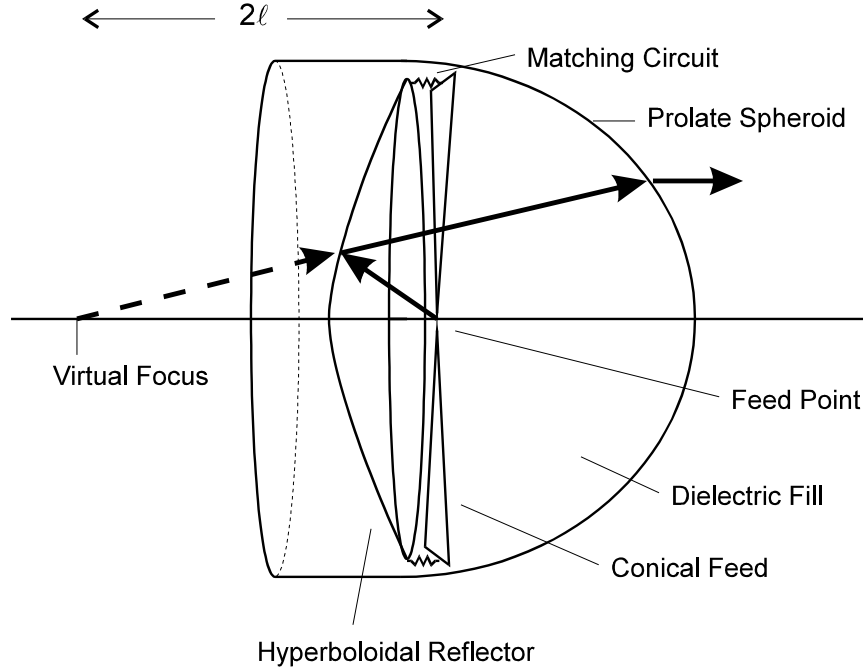


Figure 3.1. ReLIRA with Planar Reflector and prolate spheroidal Lens. (Two-arm version shown.)

Let us now provide the equations of the hyperboloid. In the  $\Psi$ - $z$  plane the equation of the surface is derived by considering the lengths of the two ray paths shown in Figure 3.2. Thus, from transit-time considerations we have

$$\begin{aligned} r_1 + (2\ell - r_2) &= 2(\ell - a) \\ r_2 &= r_1 + 2a \end{aligned} \quad (3.1)$$

Let us expand  $r_1$  and  $r_2$  in their  $r$  and  $\Psi$  components as

$$\begin{aligned} r_1^2 &= (\ell - z)^2 + \Psi^2 \\ r_2^2 &= (\ell + z)^2 + \Psi^2 \end{aligned} \quad (3.2)$$

where  $\Psi$  is again the radial cylindrical coordinate. Thus, we have

$$\sqrt{(\ell+z)^2 + \Psi^2} = \sqrt{(\ell-z)^2 + \Psi^2} + 2a \quad (3.3)$$

After squaring both sides and simplifying, we obtain

$$\frac{z\ell}{a} - a = \sqrt{(\ell-z)^2 + \Psi^2} \quad (3.3)$$

Once again, we square both sides and simplify, obtaining the equation for a hyperbola,

$$\frac{z^2}{a^2} - \frac{\Psi^2}{\ell^2 - a^2} = 1 \quad (3.4)$$

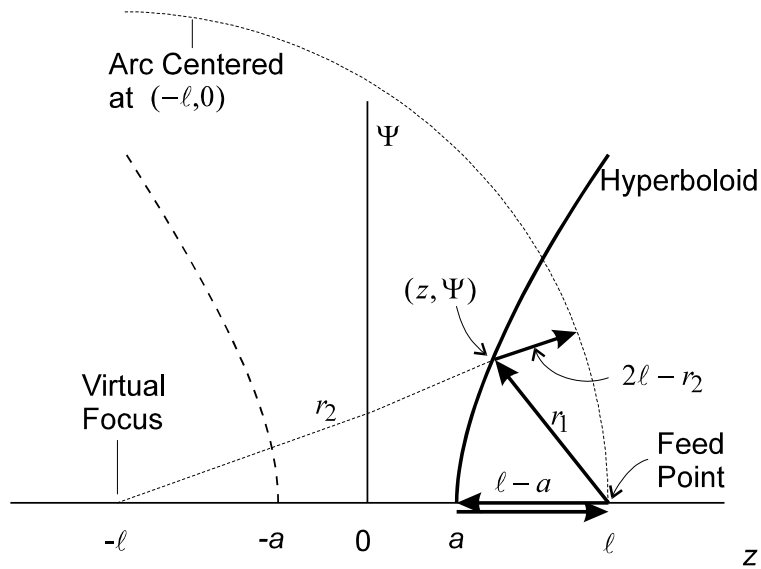


Figure 3.2. Geometry for the hyperboloid reflector, used for converting a spherical wave centered at  $(\ell, 0)$  into another spherical wave centered at  $(-\ell, 0)$ .

After making the substitution

$$b = \sqrt{\ell^2 - a^2} \quad (3.6)$$

we obtain the more usual form of the hyperbola as

$$\frac{z^2}{a^2} - \frac{\Psi^2}{b^2} = 1 \quad (3.7)$$

with foci located at  $(\pm \ell, 0)$  and  $x$ -intercepts at  $(\pm a, 0)$  [26]. The feed point is located at one focus of the hyperbola, and the virtual focus is located at the other focus of the hyperbola.

It is interesting to note that either sheet of the hyperboloid shown in Figure 3.2 could be used for the reflector, and one can think of advantages for using each. If one uses the sheet closest to the feed point, the antenna is more compact, and the wave travels less distance through a possibly lossy dielectric medium. On the other hand, by using the sheet furthest away from the feed point, one can lower the input feed impedance somewhat. This can be an advantage when there is a need to match a low-impedance source to a higher-impedance antenna.

Once the hyperboloid has been specified, it is then trivial to specify the prolate spheroid lens, using the techniques of the previous section. All that is required is that one must align the virtual focus of the hyperboloid with that of the prolate spheroid.

Note that the design of the previous section, using a flat plate reflector, is closely related to the design described in this section, using a hyperboloidal reflector. In fact, in the limit as  $a \rightarrow 0$ , the expression for the hyperbola (eqn.(3.7)) becomes a straight line along  $z = 0$ , or a flat plate when rotated about the  $z$  axis.

The radiated field for this design is determined from the same equations as the design in the previous section. This is due to the fact that, in theory, the aperture field is the same. The value of  $f_g$  one uses in the formula can be determined from either the actual feed or the virtual feed, since both feeds must have the same characteristic impedance [24]. Furthermore, the fields incident on the lens surface are calculable using the virtual feed geometry.

#### IV. ReLIRA #3: Paraboloidal Reflector with Planar Lens

The third version of the ReLIRA we wish to discuss uses a paraboloidal reflector and a planar lens or interface. A sketch of this is shown in Figure 4.1. This is actually a trivial extension of the standard reflector IRA shown in Figure 1.1, since there is no focusing at the air/dielectric interface.

This modification to the classical design may be useful in cases where a dielectric material is needed to reinforce the structure of the antenna, or in cases where a lower feed impedance is needed. The radiated field is equal to that for the classical reflector IRA, multiplied by the transmission coefficient, as described in Section II. Note that the transmission coefficient correction, which was only approximate before, is now exact because the incident field is everywhere normal to the interface.

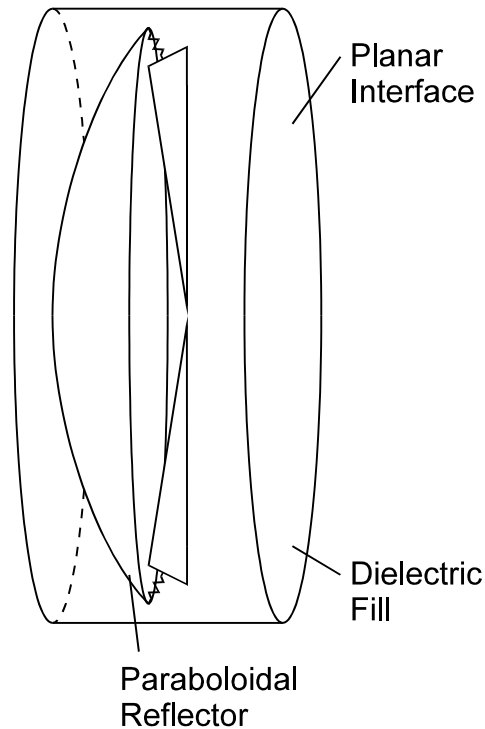


Figure 4.1. A ReLIRA with a paraboloidal reflector and a planar interface. (Two-arm version shown).

## V. Split IRA (SPIRA)

The Split IRA (SPIRA) is a technique for placing two half IRAs in close proximity, in order to implement separate transmit and receive antennas in a compact design. To implement the design, each of the two half IRAs share a thick ground plane, though which feed cables are run. Any of the designs discussed in this paper, or any of the classical reflector or lens IRA designs could be implemented in such a fashion. An example of such a design, using an ReLIRA with a planar reflector and prolate spheroidal lens is shown in Figure 5.1.

An interesting feature of such a device is that one can achieve a very low feed impedance with such a design. By using two arms for each half, the feed impedance is typically  $100\ \Omega$  in air. If the dielectric material has a relative dielectric constant of four, then the input impedance is  $50\ \Omega$ , a convenient impedance for matching to a source. In addition, this is a single-ended impedance, so it matches well to a coaxial cable input.

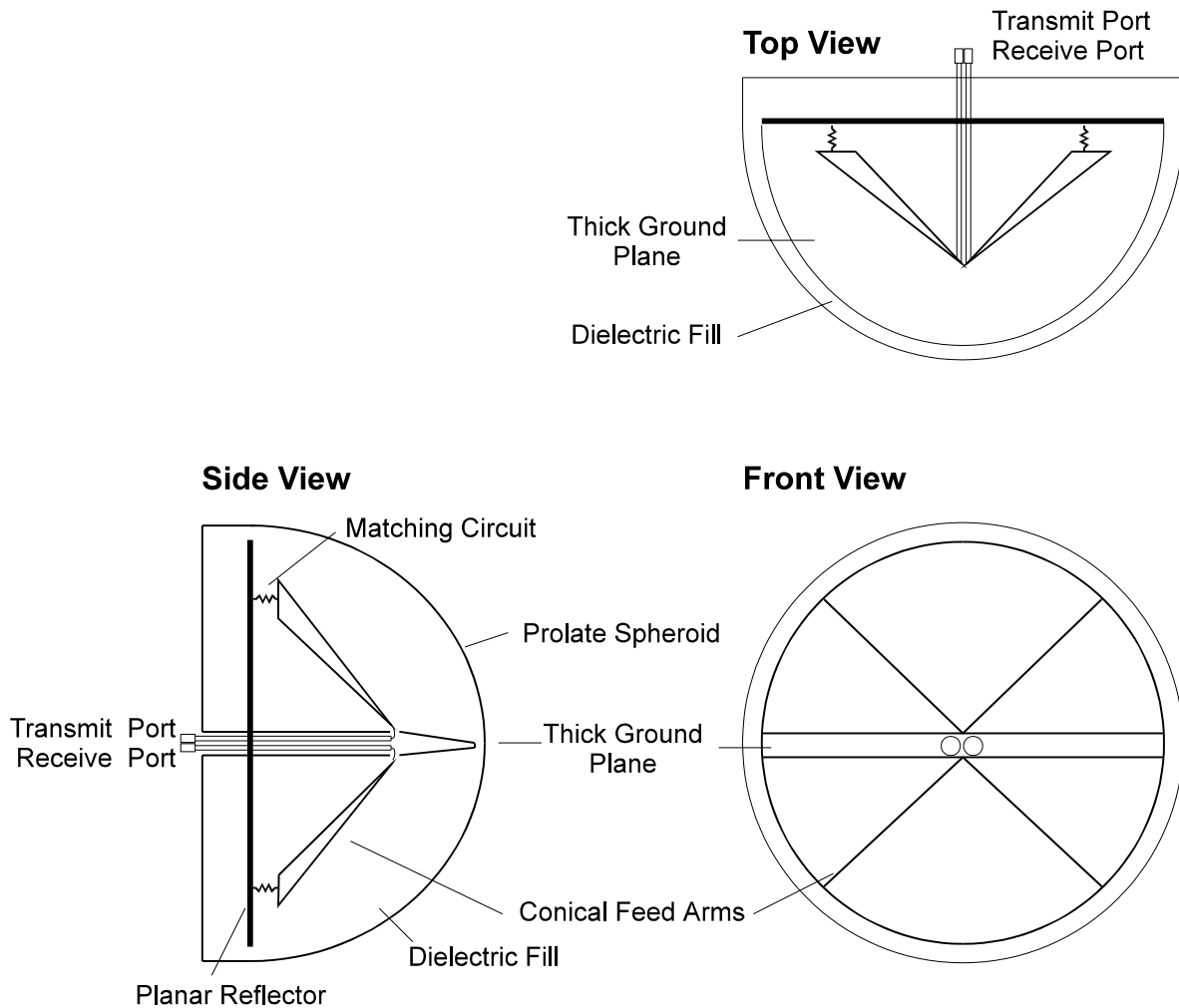


Figure 5.1. An example of a SPIRA, using a flat plate reflector and a prolate spheroidal lens. (Four-arm version is shown.)

The field radiated from such an antenna has been described in detail in Section II of this note. The only change is that the radiated field must be divided by two, since we are using only half an antenna at a time. In addition, one must adjust the feed impedance if one is using a four-arm configuration instead of a two-arm configuration.

Finally, we note that we may want to tilt the two halves of the antenna slightly toward each other, as shown in Figure 5.2. The effect of this will be to focus the antenna pair somewhere in the near field. The angle between the two halves can then be adjusted depending upon the expected distance to the object. Alternatively, one can focus in the near field by changing one or both of the reflecting or refracting surfaces to focus at a desired distance.

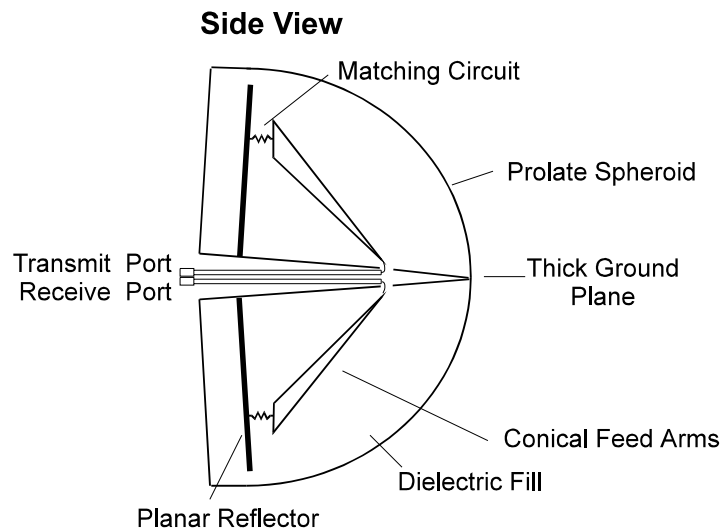


Figure 5.2. SPIRA adjusted for detecting an object in the near field.

## VI. Cassegrain IRA (CasIRA)

The Cassegrain IRA (CasIRA) is related to the classical Cassegrain reflector. Thus, there is a hyperboloidal subreflector, and a paraboloidal main reflector. A sketch of a CasIRA is shown in Figure 6.1. In addition to the symmetrical version shown, it is also possible to envision an offset design, to help avoid feed blockage. One can find additional information on the classical Cassegrain reflector in [25].

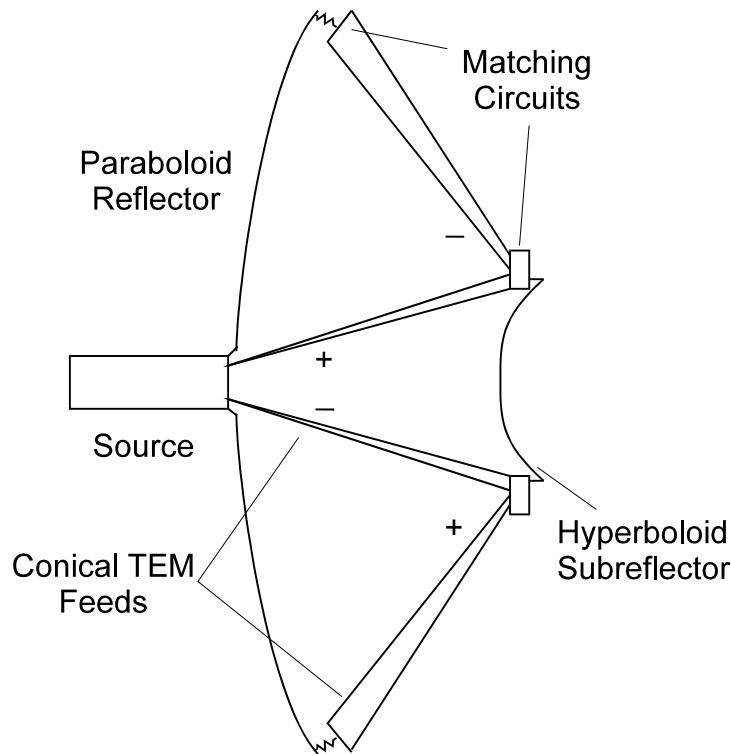


Figure 6.1. The Cassegrain IRA (CasIRA). (Shown in a two-arm version.)

With this design, one hopes to attain a more compact design than what is possible with a classical IRA. This may be most useful for radiating a high-voltage, fast risetime source, which does not allow the cable balun techniques described in [4]. For low-voltage sources, one might consider instead using a classical reflector IRA design with a short  $F/D$  ratio.

There remain a number of outstanding issues related to this antenna. First, it is not clear how to design the matching circuits shown in Figure 6.1. Ideally, one would like to invert the current on the second pair of feed arms, after reflecting off the hyperboloidal subreflector. We expect that it is easier to accomplish this at high frequencies than at lower frequencies, since we must use a passive matching circuit. If we fail to invert the low-frequency current after reflection, then the low-frequency field is oriented in the direction opposite to the high-frequency field, and this may cause some undesired complex behavior at intermediate frequencies.

Whether or not one can build a low-frequency inverter to handle this problem is at the moment quite speculative.

An additional problem arises because only the center portion of the wave is reflected. Because of this, a pure TEM wave does not exist after the first reflection. The effect of the “non-TEM” portion of the wave is unknown. Additional detail on this design will have to wait for a later paper.

## **VII. Concluding Remarks**

We have found a number of new IRA configurations that take advantage of two reflecting or refracting surfaces. These new configurations may be useful in situations where the input impedance must be kept low, or to achieve a compact design. In situations where severe mechanical stress is anticipated, designs using a solid dielectric medium may provide additional mechanical stability as well.

## **Acknowledgments**

We would like to thank Dr. Kwang Min of Wright Laboratory, for providing helpful discussions and encouragement of this work. We would also like to thank Dr. Gary D. Sower, of EG&G, Inc., who previously suggested an antenna closely related to the Split IRA.

## References

1. C. E. Baum, Radiation of Impulse-Like Transient Fields, Sensor and Simulation Note 321, November 1989.
2. C. E. Baum and E. G. Farr, "Impulse Radiating Antennas," in *Ultra Wideband/Short-Pulse Electromagnetics*, edited by H. L. Bertoni et al, Plenum Press, New York, pp. 139-147, 1993.
3. E. G. Farr, C. E. Baum, and C. J. Buchenauer, "Impulse Radiating Antennas, Part II," to be published in the *Proceedings of the 1994 Ultra-Wideband/Short-Pulse Electromagnetics Conference*, April 1994, New York, Plenum Press.
4. C. E. Baum, Configurations of TEM Feed for an IRA, Sensor and Simulation Note 327, April 1991.
5. C. E. Baum, Aperture Efficiencies for IRAs, Sensor and Simulation Note 328, June 1991.
6. E. G. Farr, Analysis of the Impulse Radiating Antenna, Sensor and Simulation Note 329, July 1991.
7. C. E. Baum, General Properties of Antennas, Sensor and Simulation Note 330, July 1991.
8. E. G. Farr and C. E. Baum, Prepulse Associated with the TEM Feed of an Impulse Radiating Antenna, Sensor and Simulation Note 337, March 1992.
9. E. G. Farr and C. E. Baum, A Simple Model of Small-Angle TEM Horns, Sensor and Simulation Note 340, May 1992.
10. C. E. Baum, Circular Aperture Antennas in Time Domain, Sensor and Simulation Note 351, November 1992.
11. E. G. Farr, Optimizing the Feed Impedance of Impulse Radiating Antennas, Part I: Reflector IRAs, Sensor and Simulation Note 354, January 1993.
12. E. G. Farr and C. E. Baum, The Radiation Pattern of Reflector Impulse Radiating Antennas: Early-Time Response, Sensor and Simulation Note 358, June 1993.
13. E. G. Farr and C. J. Buchenauer, Experimental Validation of IRA Models, Sensor and Simulation Note 364, January 1994.
14. D. V. Giri and C. E. Baum, Reflector IRA Design and Boresight Temporal Waveforms, Sensor and Simulation Note 365, February 1994.
15. E. G. Farr, Off-Boresight Field of a Lens IRA, Sensor and Simulation Note 370, October 1994.

16. C. E. Baum, Variations on the Impulse-Radiating-Antenna Theme, Sensor and Simulation Note 378, February 1995.
17. C. E. Baum and A. P. Stone, *Transient Lens Synthesis: Differential Geometry in Electromagnetic Theory*, Taylor and Francis, New York, 1991.
18. C. E. Baum and A. P. Stone, "Transient Lenses for Transmission systems and Antennas," pp. 211-219 in H. L. Bertoni et al (eds.), *Ultra Wideband/Short-Pulse Electromagnetics*, Plenum Press, New York, 1993.
19. C. E. Baum, J. J. Sadler, and A. P. Stone, A Prolate Spheroidal Uniform Isotropic Dielectric Lens Feeding a Circular Coax, Sensor and Simulation Note 335, December 1991.
20. C. E. Baum, J. J. Sadler, and A. P. Stone, Uniform Isotropic Dielectric Equal-Time Lenses for Matching Combinations of Plane and Spherical Waves, Sensor and Simulation Note 352, December 1992.
21. C. E. Baum, et al, A Uniform Lens for Launching a Spherical Wave into a Paraboloidal Reflector, Sensor and Simulation Note 360, July 1993.
22. C. E. Baum, Low-Frequency -Compensated TEM Horn, Sensor and Simulation Note 377, January 1995.
23. E. G. Farr and C. E. Baum, A Canonical Scatterer for Transient Scattering Range Calibration, Sensor and Simulation Note 342, June 1992.
24. C. E. Baum and E. G. Farr, Hyperboloidal Scatterer for Spherical TEM Waves, Sensor and Simulation Note 343, July 1992.
25. Y. Rahmat-Samii, Reflector Antennas, Chapter 15 in Y. T. Lo and S. W. Lee (editors), *Antenna Handbook*, Van Nostrand Reinhold, 1988.
26. G. B. Thomas, *Calculus and Analytic Geometry*, Alternate Edition, Addison-Wesley, 1972, pp. 485-493.